Atmos. Chem. Phys. Discuss., 11, 12763–12803, 2011
www.atmos-chem-phys-discuss.net/11/12763/2011/
doi:10.5194/acpd-11-12763-2011

Atmospheric Chemistry and Physics Discussions

Multi-wavelength Raman lidar observations of the Eyjafjallajökull volcanic cloud over Potenza, Southern Italy

L. Mona[1], A. Amodeo[1], G. D'Amico[1], A. Giunta[1], F. Madonna[1], and G. Pappalardo[1]

[1]Consiglio Nazionale delle Ricerche – Istituto di Metodologie per l'Analisi Ambientale (CNR-IMAA), C. da S. Loja, 85050 Tito Scalo, Potenza, Italy

Received: 15 March 2011 – Accepted: 18 April 2011 – Published: 26 April 2011

Correspondence to: L. Mona (mona@imaa.cnr.it)

Published by Copernicus Publications on behalf of the European Geosciences Union.

Abstract

Multi-wavelength Raman lidar measurements were performed at CNR-IMAA Atmospheric Observatory (CIAO) during the entire Eyjafjallajökull explosive eruptive period in April–May 2010, whenever weather conditions permitted.

A methodology for volcanic layer identification and accurate aerosol typing has been developed on the basis both of the multi-wavelength Raman lidar measurements and EARLINET measurements performed at CIAO since 2000. The aerosol mask for lidar measurements performed at CIAO during the 2010 Eyjafjallajökull eruption has been obtained. Volcanic aerosol layers have been observed in different periods: 19–22 April, 27–29 April, 8–9 May, 13–14 May and 18–19 May. A maximum aerosol optical depth of about 0.12–0.13 was observed on 20 April, 22:00 UTC and 13 May, 20:30 UTC. Volcanic particles have been detected both at low altitudes, in the free troposphere and in the upper troposphere. Intrusions into the PBL have been revealed on 21–22 April and 13 May. In the April–May period Saharan dust intrusions typically occur in Southern Italy. For the period under investigations, a Saharan dust intrusion was observed on 13–14 May: dust and volcanic particles have been simultaneously observed at CIAO both at separated different levels and mixed within the same layer.

Lidar ratios at 355 and 532 nm, Ångström exponent at 355/532 nm, backscatter related Ångström exponent at 532/1064 nm and particle linear depolarization ratio at 532 nm measured inside the detected volcanic layers have been discussed. The dependence of these quantities on relative humidity (*RH*) has been investigated by using co-located microwave profiler measurements. The particle linear depolarization ratio increasing with *RH*, lidar ratio values at 355 nm around 80 sr, and values of the ratio of lidar ratios greater than 1 suggest the presence of sulfates mixed with continental aerosol. Lower lidar ratio values (around 40 sr) increasing with *RH* and values of the ratio of lidar ratios lower than 1 indicate the presence of some aged ash inside these sulfate layers.

1 Introduction

On 14 April 2010 Eyjafjallajökull, a small Iceland's ice cap, entered an explosive eruptive phase after an effusive eruptive period started in March 2010. This medium-sized eruption (Petersen, 2010) caused an enormous disruption to air travel across western and northern Europe, because the volcano explosive power was sufficient to inject ash directly into the Jet Stream, located just over the volcano location, so that the Jet Stream carried the ash directly in northern Europe free troposphere, into one of the busiest airspace in the world. The explosive eruptive period lasted until 21 May 2010, with variable intensity, emission of material and plume height (Langmann et al., 2011).

Since the first explosive eruption of Eyjafjallajökull volcano on 14 April 2010, aerosol scientific community has largely been focused on the monitoring and study of the volcanic cloud. EARLINET, the European Aerosol Research Lidar NETwork, has been performed almost continuous measurements since 15 April 2010 in order to follow up the evolution of the volcanic cloud generated from the eruption of the Eyjafjallajökull volcano. EARLINET measurements have been performed accordingly to alerts distributed by CNR-IMAA based on the model calculations of the ash dispersion provided by the VAAC (Volcanic Ash Advisory Center) and EURAD (EURopean Air Pollution Dispersion). Almost the whole European continent was affected by the arrival of the volcanic cloud: UK, Germany and France had reduced visibility and volcanic particles from a very low altitude up to the upper troposphere for almost the whole 2010 Eyjafjallajökull eruptive period (Pappalardo et al., 2010a; Emeis et al., 2010; Flentje et al., 2010; Schumann et al., 2011); Italy and Greece were reached by the cloud around 20 April when the cloud after passing over Central Europe passed the Alps; the volcanic cloud was transported over the Iberian Peninsula moving then towards East, reaching again Italy and Greece (Pappalardo et al., 2010a). First studies concerning the large amount of volcanic particles observed over Central Europe during the volcanic event based on remote sensing observations have already been published in the peer-reviewed literature (Ansmann et al., 2010; Flentje et al., 2010; Emeis et al., 2010; Gasteiger et

ACPD
11, 12763–12803, 2011

al., 2010; Schumann et al., 2011). Nowadays, there is still a lack of information related to the Eyjafjallajökull plume observations in Southern Europe. Anyway, the arrival of the volcanic cloud in the Mediterranean region is particularly interesting for several reasons. Firstly, the large distance from the emitting source and the low amount of aerosols reaching this area (if compared to Central Europe) make the observations of the volcanic cloud in Mediterranean region useful and necessary for the evaluation both of model forecasts (e.g. Matthias et al., 2011) and a posteriori models (e.g. Stohl et al., 2011) at border conditions. Secondly, the observations at locations far away from the source allow us to investigate any modification in aerosol properties occurred during the transport as well as the occurrence of mixing processes across the European continent. In addition, Saharan dust intrusions in Southern Europe are typical in Spring and Summer thus offering an opportunity to study the differences and mixing of volcanic aerosols with desert dust particles. Finally, it is worth considering that since the Mediterranean is an almost closed basin, the volcanic plume arrived, even if less intense than in Central and Northern Europe, could affect the Mediterranean ecosystem.

In this paper, we are presenting and discussing the observations concerning the Eyjafjallajökull volcanic particles performed at CNR-IMAA, Potenza, Southern Italy (40°36′ N, 15°44′ E, 760 m a.s.l.).

CNR-IMAA is an EARLINET core station due to its long-term observations (it has been participating in the network since its beginning in 2000) and its state-of-art multi-wavelength Raman lidars. Moreover, the CNR-IMAA runs an advanced observatory, named CIAO (CNR-IMAA Atmospheric Observatory), equipped with the state-of-the-art instruments for the ground-based remote sensing of aerosol, water vapour and clouds (Madonna et al., 2010a). Finally, the first Raman lidar measurements of volcanic aerosol in troposphere was performed during the 2002 Etna volcanic eruption right at CNR-IMAA (Pappalardo et al., 2004) and these observations were object of a detailed study based on an integrated approach between lidar observations and transport modeling (Villani et al., 2004). Taking advantage both of this expertise and the

ACPD
11, 12763–12803, 2011

long-term database of lidar observations collected at CIAO, a methodology for identifying the volcanic aerosol layer in the aerosol vertical profile time-series has been developed. Lidar measurements performed during the Eyjafjallajökull eruptive period are shortly described in Sect. 2. The methodology for aerosol masking is described in Sect. 3. The aerosol masks for the observations collected during the 15 April–20 May 2010 period are reported in Sect. 4 which also reports results in terms of the aerosol optical properties of the identified volcanic aerosol layers. Finally, a summary is given.

2 Lidar measurements

The current study mainly relies on lidar measurements performed by PEARL (Potenza EArlinet Raman Lidar), the multi-wavelength lidar system for tropospheric aerosol characterization designed and operated by CNR-IMAA since August 2005 (Mona et al., 2009). This system is an upgrade of a pre-existing Raman lidar system for tropospheric aerosol study which has been operative since the EARLINET beginning in 2000 (Mona et al., 2006b). PEARL measures the radiation elastically backscattered from the atmosphere at three laser wavelengths (355 nm, 532 nm and 1064 nm), the N_2-Raman shifted radiation backscattered at 387 nm and 607 nm, and the perpendicular and the parallel polarized components of the 532 nm backscattered light (with respect to the linearly polarized laser beam direction). Simultaneous aerosol extinction and backscatter profiles at 355 and 532 nm are retrieved with the combined elastic-Raman retrieval (Ansmann et al., 1992). The aerosol backscatter at 1064 nm is retrieved through an iterative procedure (Di Girolamo et al., 1999), with a lidar ratio profile selected on the basis of the 3 backscatter +2 extinction (3+2 in the following) measurements performed at CIAO. The particle linear depolarization ratio profile at 532 nm is retrieved by using the "0°-calibration" technique as described in Freudenthaler et al. (2009). More technical details of PEARL set-up and retrieved products can be found in Madonna et al. (2010a) and Mona et al. (2009).

ACPD
11, 12763–12803, 2011

CIAO also runs MUSA (MUltiwavelength System for Aerosol), a compact and transportable multi-wavelength lidar system that is one of the reference systems used in the frame of the EARLINET Quality Assurance program. Because of the preparation for the lidar intercomparison campaign scheduled for May 2010 in Madrid (Spain) in the frame of the EARLINET-ASOS project, MUSA was not operational during the volcanic event. On 10 May 2010, the campaign was finally delayed to October because of the Eyjafjallajökull eruption. This time frame was not sufficient to obtain MUSA measurements in a systematic way during the volcanic event, therefore the results showed in this paper are based only on PEARL measurements.

In order to meet both scientific and public interests in this volcanic eruption, lidar measurements were performed at CIAO during the alert periods, whenever weather conditions permitted, accordingly to EARLINET observational strategy established for this volcanic eruption event (Pappalardo et al., 2010b). There were two main periods of volcanic-cloud transport over Europe (Pappalardo et al., 2010a): 15–30 April, when wind transported the emitted material over Central Europe and then towards the South-Southeast; after 5 May, when most of the Eyjafjallajökull volcano emissions reached almost directly Western Europe and then were transported towards Italy, Greece and the Balkans.

From 15 April, when the first alert was sent, until 19 April lidar measurements could not be performed at CIAO due to low clouds and rain. Since then, PEARL ran almost continuously until the evening of 22 April with some long breaks due to low clouds. During this period the arrival of volcanic ash was forecast over Northern and Central Europe and, after that, a feeble transport of ash beyond the Alps. Intense rain did not permit measurements from the evening of 22 April until 25 April, when lidar measurements started again. Observational period continued until 30 April, limited to relatively short temporal windows without low clouds or rain. In this period, desert dust arrived over Southern Europe followed by a change in the wind direction with air masses coming from North-Eastern Europe. In the 25–30 April period the circulation over Europe changed: wind from Northern Europe could have transported material emitted by the

ACPD
11, 12763–12803, 2011

Eyjafjallajökull volcano over Western Europe and then over Italy and Greece. This main situation lasted for the following days, when Saharan dust intrusions over Southern Europe also occurred. A possible arrival of volcanic cloud over Northern Italy was forecast for 8 May. Accordingly, lidar measurements were performed from 8 May, 20:00 UTC till 11 May, 02:00 UTC, with some interruptions because of fog and low clouds. CIAO lidar ran measurements from 12 May, 12:00 UTC, till 15 May, 01:00 UTC, when a shower forced a sudden stop. The last special measurements performed for the Eyjafjallajökull volcano started as soon as weather conditions permitted, on 18 May, 06:00 UTC, and continued until 19 May, 11:00 UTC.

Quick-looks of time series of elastically backscattered lidar signals were made available in near real time at CNR-IMAA web site (www.imaa.cnr.it) in order to satisfy national and international requests for information on the volcanic cloud detection for both scientific and public aims. A link to an EARLINET quick-look web-page (www.earlinet.org) allowed an easy and fast overview of the aerosol layers over Europe during the whole period. In addition, a daily report of CIAO volcanic cloud observations was delivered and collected together with those of the other EARLINET stations summarizing relevant information on volcanic cloud over Europe. Regarding CIAO observations, a preliminary quick analysis showed 4 periods that could be affected by the arrival of volcanic particles: 19–22 April, 27–29 April, 8–10 May, 12–14 May and 18–19 May.

3 Methodology

A big effort was made at CIAO in order to collect as large database as possible of volcanic-related lidar observations. Periods probably affected by the arrival of emitted volcanic materials over Italy were identified by a preliminary near-real time inspection of these data. However, a dedicated and specific analysis is needed in order to investigate the time and range resolved occurrences of volcanic cloud observations. Lidar measurements are particularly effective for the near real time identification of high

ACPD
11, 12763–12803, 2011

aerosol content, because the false image color map of the lidar range corrected signals, quickly available, provides a snapshot of the temporal evolution of the aerosol content as a function of the altitude (see Fig. 1 for example) where warm colors indicate a high aerosol content. The aerosol typing, instead, is not so easy to be performed. There are different automated methods, such as that used for the CALIPSO retrievals (Liu et al., 2010) based on modeled aerosol properties and multi-year AERONET experimental findings which takes into account the typical size distributions and refractive indices of the aerosol types chosen. This kind of typing algorithms is highly performing for the providing of typically reliable results in near-real time. However, it relies on the idea that the whole range of possibilities in terms of optical properties had already been measured and characterized for each aerosol class. Therefore, these algorithms are not feasible for particular scenarios such as tropospheric volcanic clouds due both to the specificity of each volcanic eruption in terms of emitted particles and the overall scarcity of observations related to this kind of event. On the contrary, the multi-wavelength Raman lidar has been widely demonstrated to be an effective tool for aerosol characterization thanks to its capability to measure aerosol optical parameters independently and directly: lidar ratio in UV and visible ranges, Ångström exponents for the extinction and backscatter coefficients and, typically, the depolarization ratio. In particular, many studies have been carried out within EARLINET for the aerosol characterization both of different aerosol types at single stations (e.g. Müller et al., 2007) and the same aerosol type at different locations (e.g. Papayannis et al., 2008). The main result is that significant differences are found also for the same type of aerosol because of the variability in aerosol optical and physical properties at the source, modification processes occurred during the transport and the mixing with other aerosol types. Moreover, it has been shown that a careful analysis based on lidar observations, air-mass backtrajectories and modeling tools is needed for a detailed classification of the observed aerosols (e.g. Mona et al., 2006b; Müller et al., 2009; Villani et al., 2006; Pappalardo et al., 2010c).

ACPD
11, 12763–12803, 2011

The aim of this paper is to describe the temporal and vertical evolution of the volcanic aerosol content over a lidar station located far away from the volcano, where the amount of volcanic aerosol is much lower than that observed in Central Europe (e.g. Schumann et al., 2011; Ansmann et al., 2010; Gastegeir et al., 2010), and in a period in which Saharan dust intrusions are often observed in Southern Europe. Therefore, a detailed analysis is needed both for the typing of aerosol layers and the investigation of aerosol mixing processes.

An appropriate methodology has been developed by following a step procedure consisting of: (i) the identification of particle layers; (ii) cloud vs aerosol discrimination (iii) aerosol typing through the investigation of intensive properties measured by multi-wavelength Raman lidar and models and back-trajectory analysis.

Below, the methodology for a detailed and accurate aerosol typing is described in depth by means of an exhaustive example: the 12–14 May observations have been selected because they are characterized by a high variability with the presence of both wide and thin intense aerosol layers, cirrus, and sparse low clouds. The general atmosphere situation corresponding to this measurement period is characterized both by desert dust outbreaks over the Central Sahara and mean wind typically coming from the South East and therefore rich in dust particles. On 13 May morning, a sort of interruption in this transport seems to occur with air masses mainly coming from Northern Europe after passing over the Iberian Peninsula.

Figure 1 reports the temporal evolution of the range corrected lidar signal measured at 1064 nm at CIAO in the 12–14 May period. The signature of a strong particle layer about 1–1.5 km deep is evident at the beginning of the measurement record decreasing in altitude from 5 to 3 km a.s.l. In the early morning of 13 May, the arrival of a feeble layer is distinguishable at 6 km, falling down in the following hours and becoming an intense but very thin layer located around 2–2.5 km from the afternoon of 13 May until the early morning of 14 May. Frequent and short intense lidar returns are evident below 2 km between 13 May, 12:00 UTC, and 14 May, 04:00 UTC, when measurements were interrupted because of low clouds and light rain. Measurements started again when

ACPD
11, 12763–12803, 2011

rain stopped. Aerosol layers were present up to 6 km on 14 May from 09:00 UTC to 23:00 UTC, when low clouds followed by intense rain forced the measurement stop.

3.1 Layers identification

An algorithm has been implemented for the identification of layers above the PBL. The main concept is that features can be identified through the first derivative of the particle backscatter profile. Other methods are reported in literature (e.g. Steyn et al., 1999; Wang and Sassen, 2008) and their enhanced capability in different conditions is shown. However, the results obtained by using all these methods agree within the experimental errors. Respect to commonly used procedures for aerosol/cloud identification (e.g. Morille et al., 2007; Vaughan et al., 2004), the advantage we have is that of starting from calibrated backscatter profiles, whose high quality is certified by the EARLINET quality assurance program (Böckmann et al., 2004; Pappalardo et al., 2004), rather than from quasi raw signals (namely the range corrected signals). This makes it possible to overcome problems related to the normalization processes applied in automated methods based on range corrected signals.

However, since the derivative is an ill-posed procedure which generally works well only where the signal to noise ratio is sufficiently high, a smoothing procedure is needed. It is well-known that smoothing procedures can produce some distortions along the signals, so that particular care has to be taken in the smoothing procedure selection. A second-order Savitsky-Golay filter is applied on the differential, since it seems to be effective for the preservation of the vertical structures without introducing any artificial features (Pappalardo et al., 2004). The number of points is progressively increased in order to avoid false-layer identifications due only to the noise affecting the signals. However, a maximum of 1000 m is fixed for the effective vertical resolution evaluated by using the Rayleigh criterium (Pappalardo et al., 2004).

This method for the identification of layers can be applied only in regions where the relative statistical error on backscatter profile is sufficiently low. Tests performed on several EARLINET station data have made it possible to identify 30% as a reasonable

ACPD
11, 12763–12803, 2011

limit for the application of the derivative method. In the altitude region characterized by a relative error on aerosol backscatter coefficient higher than 30%, layers are not identified through the derivative method, but as those regions where the aerosol backscatter scattering ratio is higher than a pre-defined threshold. In particular, particle layers should correspond to a scattering ratio significantly higher than the aerosol background condition as defined on the basis of the long-term aerosol observations performed at CIAO since 2000. A scattering ratio threshold is fixed as the observed aerosol background value, evaluated in the 6.5–8.5 km altitude range, typically not affected by an intense particle transport. This resulted in a threshold for the scattering ratios of 1.02, 1.05 and 1.35 at 355, 532 and 1064 nm, respectively. Particle layers are identified as altitude regions where the scattering ratio is higher than the defined threshold plus the scattering ratio absolute statistical error.

The layer identification is performed above the PBL top altitude calculated by using the procedure established within EARLINET (Matthias et al., 2004). In this way, layers consisting of transported aerosols (like Saharan dust and volcanic aerosol) can be identified. Regarding the PBL region, intrusions from upper level layers would lead to a mixing of local aerosol (typically confined in the PBL) with transported aerosol, in this case volcanic aerosols. These situations will be identified on the basis of the temporal evolution of the layers and modification of aerosol optical properties in the PBL region.

Finally, only the altitude ranges where the statistical error on backscatter coefficient is lower than 50% are considered in this spatio-temporal evolution study, in order to provide reliable information on the aerosol masking.

A compromise between the high temporal resolution available for the backscatter profiles and a longer time average, needed to reduce the statistical error, is necessary. A temporal average of 1 h is chosen in order to be able to draw a direct comparison with models that typically run every 6 h and mainly provide data every hour (e.g. Matthias et al., 2011).

The aerosol backscatter coefficient at 1064 nm is used for the layering taking advantage of the stronger sensitivity to the aerosol structures at this wavelength respect

ACPD
11, 12763–12803, 2011

to visible and ultraviolet ones. The iterative procedure reported in Di Girolamo et al. (1999) is applied for the 1064 nm backscatter retrieval, with lidar ratio values selected on the basis of the 3+2 measurements performed at CIAO. The effective vertical resolution is chosen each time as the best possible to optimize relative error and vertical profiling capability, and it is typically 60 m for the cases under investigation. The routine for the particle layer identification runs on individual backscatter profile. As final step, a consistency check is performed on the resulting layering temporal evolution.

Figure 2 reports an example of single profile particle layer identification. The base and top of each layer are indicated as dotted and solid horizontal lines, respectively. A detailed layering structure characterization is obtained up to the upper troposphere, indicating the presence of an aerosol load higher than what is typically measured at CIAO up to 12 km a.s.l. The derivative technique (applied below the 30% error limit, i.e. black region in the plot) allows us to characterize the internal structure of multi-stratified complex aerosol layers, identifying 5 distinct aerosol layers above the PBL top up to 9 km altitude region on the basis of the aerosol backscatter gradient analysis. At upper levels thin and sparse layers are identified as exceeding the threshold on the scattering ratio. This is a trace of the presence of a low amount of aerosol at these altitudes. However, longer time averages, or a time series analysis, would allow us to better describe the upper level particle layers.

3.2 Clouds identification

After the identification of the particle layers, the type of the observed particles has to be identified. A first preliminary discrimination is carried out between aerosol and clouds. Cirrus clouds are identified mainly on the basis both of their temporal dynamical evolution (Mona et al., 2007) and the almost neutral backscatter spectral dependence, because hydrometeors are much larger than the lidar detection wavelength. Following EARLINET protocol, low clouds are removed from the backscatter profile evaluation by the eye-inspections of single raw data. The analysis of the temporal evolution of the

ACPD
11, 12763–12803, 2011

retrieved aerosol backscatter profile is an additional check of the appropriateness of low cloud removing procedure.

For the 12–14 May case, low clouds prevented measurements for about 6 h. The calculation of aerosol backscatter profile is not always possible for this measurement run: on 12 May the presence of a middle cloud just above the intense aerosol layer extending up to about 4 km did not permit the normalization needed for aerosol backscatter retrieval for more than 10 h, and 4 aerosol backscatter profiles in the time series cannot be retrieved for the presence of low altitude and strongly extinguishing clouds. A total of 34 1-h aerosol backscatter profiles were calculated for the event covering the 13 May, 04:00 UTC–14 May, 21:00 UTC time window. For these profiles, there is a large percentage of skipped files for low cloud contamination. In particular, on average 46% of the files were skipped for a total amount of about 16 h.

3.3 Aerosol typing

In order to study the origin and the nature of the aerosol layers identified through the procedure described in 3.1, backward trajectory analyses and model outputs are used. In particular, 10-day HYSPLIT backtrajectory analysis provided by NOAA (Draxler and Rolph, 2011) is used because of its larger flexibility. Actually, 3 arrival altitudes can be set by the users on the basis of specific needs, and the arrival time can be chosen with a 1-h resolution. These options make the HYSPLIT backtrajectory analysis very flexible for the aerosol typing in an integrated study with high vertical and temporal resolution lidar data. The use of backtrajectory analysis for the identification of aerosol origin is nowadays well recognized, especially for large source areas such as desert regions. Deeper attention should be paid in the presence of an almost punctual source, as in the case of volcanic eruptions and in particular for observations performed at long distances from the source, because the particle position uncertainty increases with the trajectory length, with lower uncertainty for higher wind speed (Stohl, 1998). For potential volcanic eruption cases, the stability of the aerosol typing is checked by slightly changing both arrival altitudes and times. In addition, other backtrajectory analyses are

ACPD
11, 12763–12803, 2011

used as further checks: 4-day backward trajectories provided by the German Weather Service (DWD) at each EARLINET lidar station for two arrival times per day and for six arrival pressure levels between 200 and 975 hPa (Stohl, 1998); FLEXTRA trajectory model (Stohl et al., 1995) provided for each EARLINET site every 6 h at 1500, 3000 and 5000 m as arrival altitudes; and Trajectory Analysis developed by the Atmospheric Chemistry and Dynamics Branch of the NASA/Goddard available for each AERONET site at 00:00 UTC and 12:00 UTC for 8 height levels between 950 and 200 hPa (Schoeberl and Newman, 1995).

Once the particle path is identified, the occurrences of a specific event along the path is checked against both related models and satellite data, when available, in order to identify the potential aerosol source (for example desert, volcano and fires). In particular, DREAM (Dust REgional Atmospheric Model) forecasts are used for Saharan dust in terms of maps of the dust loading over the Mediterranean and dust concentration profiles over Potenza EARLINET site, both available every 6 h. The Eyjafjallajökull volcanic activity and emission heights are checked through updated reports provided by the Iceland Meteorological Office, VAAC and EURAD forecasts and dedicated studies (e.g. Langmann et al., 2011). Finally, the presence of forest fire episodes is checked by using the World Fire Atlas available at http://wfaa-dat.esrin.esa.int/, based on ATSR Active Fire Algorithm.

HYSPLIT backtrajectory analysis for the 3 main situations observed on the 12–14 May period (i.e. large and spread aerosol load at the beginning of the measurements run, a small and confined aerosol layer in the middle of the observations and a wide and spread aerosol layer observed towards the end of the measurements) are reported in Fig. 3 together with the DREAM forecast of dust concentration vertical profiles.

At 00:00 UTC on 13 May, a peak in the dust concentration is forecast extending between the ground and 6 km (Fig. 3d). At the same time, the backtrajectories (Fig. 3a) show at low altitudes the arrival of air masses passing over West Sahara very close to the surface in agreement with the DREAM forecast. At upper levels, DREAM does not

ACPD
11, 12763–12803, 2011

Lidar observations of the Eyjafjallajkull volcanic cloud over Southern Italy

L. Mona et al.

forecast dust load and the backtrajectories pass over Africa at very high altitudes, so air masses are not rich in dust, and insist, instead, over Iceland at altitudes in agreement with the observed plumes (Langmann et al., 2011; Matthias et al., 2011).

In the following hours the situation changes significantly (see for example Fig. 3b and e) with air masses coming from North Western Europe, very close to Iceland, where both satellite images and ground-based measurements show volcanic particle presence (Pappalardo et al., 2010a; Schumann et al., 2011). On the other hand, the backtrajectory analysis shows air masses that, even if partially passing over Africa, fast increase in altitude so that the Sahara is unlikely to be the source of the observed aerosol. Finally, DREAM forecasts a low dust amount, as typically observed at CIAO in multi-year Saharan dust observations as a background level between two consecutive dust events. Therefore, the thin layer observed on 13 May can be traced to volcanic emission.

Finally, the Saharan dust component of aerosol observed on 14 May, at 12:00 UTC, has significantly increased as suggested both by the DREAM forecast and the air masses passing over the desert close to the ground (Fig. 3f and c, respectively). Moreover, the transport of volcanic aerosol from Iceland was still continuing as highlighted by the air mass reaching Potenza at about 2 km a.s.l.

Summarizing, during the 12–14 May period we have three main situations: (a) dust loading below 6 km and volcanic aerosol at upper levels, (b) volcanic aerosol and (c) dust/volcanic mixed situation.

Special attention must be paid to the transition region (in time and vertical dimensions) where the identification of the aerosol layers through the analysis of one wavelength backscatter lidar (Sect. 3.2) and the combined use of models and backtrajectories is not sufficient, and would lead to an undefined aerosol zone in the resulting aerosol mask. Because of the instability of the backtrajectory analysis in the transient regime among the different situations, which is also due to the uncertainties affecting the backtrajectory analysis, a clear identification of the aerosol typing would be impossible.

This uncertain situation occurred for example on 13 May, around 05:00 UTC, in the transient between situations (a) and (b). As example Fig. 4a and b report the back-trajectories for 3, 5 and 11 km a.s.l. for 04:00 UTC and 06:00 UTC, respectively, and Fig. 4c and d the backtrajectories for the same times but with 0.5 km differences in arrival altitudes (2.5 km, 3.5 km and 4.5 km). When comparing these figures, it is clear that small changes in time (profiles are obtained with 1 h integration time) and/or in altitudes result in large differences in the air mass travelling path both in horizontal and vertical dimensions. In cases like this, only through additional high quality range resolved measurements a reliable identification of the aerosol typing is possible. In this context the single backscatter lidar technique is not sufficient to characterize aerosol. Due to established temporal resolution, low cloud occurrences and daytime condition, Raman measurements are not available for these time slots. Moreover, by taking advantage of the dust climatology based on lidar measurements performed at CIAO and using the multi-wavelength observational capability, a reliable aerosol typing is possible. The spectral behavior of the aerosol backscatter and, in particular, its temporal evolution are used here in order to distinguish between dust and volcanic particles.

The profiles of the aerosol backscatter at 1064 nm for this uncertain situation on 13 May around 05:00 UTC, are reported in Fig. 5 together with the backscatter related Ångström exponent at 532/1064 nm. On 13 May, at 04:00 UTC, the backscatter related Ångström exponent at 532/1064 nm (in the following å(β)) has values ranging between 1.8 and 0.8 from the PBL top up to 4 km a.s.l., with a trend decreasing with the altitudes and a mean value of about 1 in agreement with the results obtained in a multi-year climatological study of Saharan dust intrusions over Potenza (Mona et al., 2006b). The same mean value is found for the 4–6 km altitude range, even if characterized by larger oscillations due to a higher statistical error. Therefore, the 2 identified layers extending between PBL and 6.4 km a.s.l. are classified as Saharan dust aerosol layers.

The å(β) profile for 05:00 UTC shows the same dependence on the altitude in the 2.1–3.2 km range with a shift toward lower values with respect to what is measured at 04:00 UTC. Between 3.2 and 6.4 km a.s.l. the aerosol backscatter profile is

ACPD
11, 12763–12803, 2011

different from the previous one, with the presence of 2 layers extending between 3.2–4.9 km a.s.l. and 5.1–6.4 km a.s.l. According to the air mass backtrajectories these altitudes could be affected by the arrival of volcanic cloud, consistently with the mean å(β) value of 0.2 which is different from values observed just before for Saharan dust. This indicates a mixing between dust and volcanic particles.

The å(β) profile measured at 06:00 UTC has, instead, a completely different altitude dependence: å(β) is almost constant (about 1) with the altitude, indicating a homogeneous layer in term of aerosol dimension up to 3.4 km a.s.l., and the corresponding backscatter profiles at 532 and 1064 nm (see Fig. 2) decrease with the altitude and without pronounced peaks, as typically happens in well mixed situations, indicating a mixing between PBL aerosol and desert dust particles. The feeble feature extending between 3.4 and 4.3 km a.s.l. is characterized by å(β) around 0.2, significantly lower than those observed in dust and in dust/local mixed aerosol, indicating the mixing with volcanic larger particles. At upper levels (up to 6.8 km), the backscatter related Ångström exponent shows different values typically close to zero, indicating, for this case, the presence of volcanic aerosol.

The result of the aerosol masking for the 13–14 May case is reported in Fig. 6, where desert dust layers are reported in orange, pink ranges denote mixing cases (local-dust and dust-volcanic) and different shades of grey, according to the mean aerosol backscatter at 1064 nm, the volcanic aerosol layers. It is worth considering that the observed particles of volcanic origin may be affected by modification processes and mixing with path-encountered air masses during the long-range transport because of the large distance between the source (volcano) and the measuring point. Cases in which a further significant aerosol source is identified (as in the case of dust on 14 May afternoon) are classified as mixed aerosols. As far as this is concerned it is worth mentioning that other different sources from volcano and Sahara desert, and correspondingly other aerosol types, are taken into account: forest fires, that, when present, are reported in green, and continental aerosol (brown). PBL aerosols and clouds and/or cirrus clouds are reported in yellow and cyan, respectively. If the origin identification of

ACPD
11, 12763–12803, 2011

the layer observed should not be possible at this stage, aerosols would be classified as unknown (purple).

4 Results

The methodology described in the previous section by detailing the 13–14 May example is applied to all the periods identified as potentially affected by the volcanic cloud: 19–22 April, 27–29 April, 08–09 May, 13–14 May and 18–19 May.

Aerosol mask for the entire April–May period is reported in Fig. 7. In Sect. 4.1, the resulting mask for each of these periods is described in depth, and optical properties are discussed as well. Finally, an overview of the volcanic aerosol optical properties is provided in Sect. 4.2.

4.1 Aerosol masks

4.1.1 19–22 April 2010

The first arrival of volcanic particles at CIAO was recorded on 19 April 2010 at 20:00 UTC, when the models did not forecast any other possible source for the observed aerosol layers and the backtrajectories showed air masses coming from Iceland and reaching Potenza. In the period 19 April, 21:00 UTC – 20 April, 21:00 UTC, the retrieval of 1-h backscatter profiles was inhibited because of low clouds. Volcanic particles were present over the whole investigated altitude range for the entire measurement period. In daytime conditions, a smaller altitude range was investigated in terms of aerosol typing respect to nigh-time conditions because of the established limit of 50% on statistical error. A mixing with PBL entrapped aerosol was observed since 21 April, 01:00 UTC, causing an increase in the PBL top up to 2.8 km a.s.l. (i.e. 2 km above the ground), which is an unusual value for night-time observations (Mona et al., 2009). At 10:00 UTC, this 2 km-deep layer splits into two sharp layers, one from the ground up

Discussion Paper | Discussion Paper | Discussion Paper | Discussion Paper |

ACPD

11, 12763–12803, 2011

Lidar observations of the Eyjafjallajkull volcanic cloud over Southern Italy

L. Mona et al.

to PBL top at 1.5 km a.s.l., and the other above the PBL up to about 3 km a.s.l. The low PBL top altitude observed at this time indicates that these mixed aerosols almost fall to the ground, in agreement with SEM analysis carried out on the PM2.5 samples collected at CIAO during the period under study (Lettino et al., 2011). At upper levels the arrival of volcanic particles was still continuing. Another intrusion into the PBL is observed at 14:00 UTC, 22 April, when the natural increasing in the PBL top due to the solar heating results in the mixing between PBL aerosol and volcanic aerosol located just above it.

A complete multi-wavelength analysis for the most significant time-windows is performed when cloud cover permits: 20 April, 21:00–23:05 UTC; 21 April, 00:29–01:30 UTC, and 21 April, 19:06 UTC – 22 April, 03:09 UTC (see Table 1 for mean values calculated within identified layers). In addition, aerosol extinction and backscatter at 355 nm are available on 19 April, at 19:53–20:36 UTC, together with the aerosol backscatter at 1064 nm. For 19 April, when there was no alert for volcanic particle arrival over Potenza, measurements at 532 nm were not available because of an internal protocol aimed at optimizing the PEARL system capability to monitor the water vapor in the framework of GRUAN (GCOS Upper-Air Reference Network) (Madonna et al., 2010a).

A lidar ratio at 355 nm of 54 sr is observed on the first volcanic cloud arrival, in agreement both with the values measured at our station for the close-by volcanic event during the 2002 Etna eruption (Pappalardo et al., 2004) and the Central Europe EARLINET measurements of Eyjafjallajökull volcanic plume (Ansmann et al., 2010). The large standard deviation of this lidar ratio value could indicate that the identified layer is not so homogeneous in terms of aerosol microphysical properties and this could be ascribed both to a small component of volcanic particles respect to the background ones and the long complex transport path (Villani et al., 2006; Mona et al., 2006a). On 20 April, the maximum peak in the aerosol backscatter at 1064 nm (3×10^{-7} m^{-1} sr^{-1}) is observed around 22:00 UTC at about 3.5 km a.s.l. At the same time, the maximum in aerosol optical depth occurred with a value of 0.13 at 355 nm. Lidar ratio values

ACPD
11, 12763–12803, 2011

calculated within the identified layers (around 2.5 and 3.5 km a.s.l.) are around 40 sr and 50 sr at 355 nm and 532 nm, respectively. The Ångström exponent (available only for the lowest of the 2 layers) of 1.4 indicates particles which are on average smaller than those observed in Central Europe (Ansmann et al., 2010). Correspondingly, the mean particle linear depolarization ratio at 532 nm is around 20%, which is significantly lower than the values around 35% measured in Germany for this volcanic event (Ansmann et al., 2010). These differences with Leipzig lidar measurements can be due both to the longer transport path and a possible contamination with continental aerosols. It is interesting to underline the low variability of lidar ratio in this case, which could indicate a more defined and homogeneous situation in terms of microphysical properties.

During the 19–22 April period, an increase in the mean particle size is observed: the backscatter-related Ångström exponent at 532/1064 nm decreases from 1.8 recorded on 20 April evening, to 1.2 during the 21–22 April night, passing through 1.3 diurnal measurement during the 21 April. Correspondingly, also the Ångström exponent decreases from 1.4 down to 1.1. On the other hand, the particle linear depolarization ratio slightly increases from 15 % up to 25% in the 19–22 April period, indicating an increase in the particle mean asphericity.

During the 21–22 April night, lidar ratio values up to 80 sr at 355 and 532 nm are observed. These values are larger than those observed in the previous phase for volcanic particles, but are also significantly larger than 37 sr at 355 nm typically obtained at CIAO (Mona et al., 2006a). The high lidar ratio and decreased Ångström exponent might be due to the hygroscopicity of the volcanic particles. This hypothesis is supported by the relative humidity measured by the microwave radiometer operative at CIAO: in the volcanic aerosols layer, a relative humidity around 20% is measured on 20 April evening, while it is around 50% on 21 April. In addition, the volcanic layer observed at 1.6–3.4 km a.s.l. is the result of the splitting of the 2 km-deep PBL: the volcanic aerosol intruded into the PBL on 21 April, around 01:00 UTC, after that the 2 km-deep PBL separated into 2 well defined layers, one confined below 1.5 km and the other extended between 1.6 and 3.4 km a.s.l. In the light of this, the 1.6–3.4 km

ACPD
11, 12763–12803, 2011

volcanic layer observed is probably affected by modification of aerosol optical properties because of the mixing with local aerosols.

4.1.2 27–29 April 2010

This event is completely different from the previous one in terms of aerosol amount and transport mechanisms. As reported above, the measurements stopped on 23–24 April due to rain, and on 25 April a strong dust event was observed. The unknown aerosol classification is reported for the observation on 27 April. Backtrajectory analysis for 27 April morning does not show any clear origin of the air masses. The limited number of hours available for the analysis as well as the availability of only diurnal measurements for this day do not allow us to take advantage either of the study of the layer temporal/vertical evolution or the Raman and multi-wavelength capabilities. On 29 April evening, however, there is the clear evidence of volcanic particle arrival at CIAO in the entire free troposphere. For this case, a peak in the aerosol backscatter coefficient at 1064 nm of about $2.3 \times 10^{-7}\,m^{-1}\,sr^{-1}$ is observed around 22:00 UTC at about 2 km a.s.l. The complete multi-wavelength analysis available for the lowest and most intense aerosol layer (2.7–3.4 km a.s.l.) indicates, also for this case, the presence of smaller and more absorbing particles than those observed in Northern Europe (Ansmann et al., 2010).

4.1.3 8–10 May 2010

Since 5 May, wind directions over Europe changed respect to the previous days, transporting the volcanic cloud almost directly over the Iberian Peninsula and then towards Italy, Greece and the Balkans. Measurements at CIAO started on 8 May accordingly to the plume dispersion forecasts. The reported methodology allows us to identify volcanic aerosol layering up to 10 km a.s.l. In particular, the most intense layer is close to the surface just above the PBL top, with a peak in the aerosol backscatter coefficient at 1064 nm of about $1 \times 10^{-6}\,m^{-1}\,sr^{-1}$ observed at about 2 km a.s.l. at 18:00–22:00 UTC.

ACPD
11, 12763–12803, 2011

Both particle linear depolarization ratio and Ångström exponents indicate the presence of particles on average larger and less depolarizing than those observed starting from 22 April night, but with similar lidar ratio values.

4.1.4 13–14 May 2010

The situation observed during this period has been described in Sect. 3, with transitions between dust intrusion, mixing between dust and volcanic particles depending on the altitude, a completely volcanic phase and again the arrival of large quantity of dust over a background of volcanic particles. For the volcanic layer, a peak of $8 \times 10^{-7}\,m^{-1}\,sr^{-1}$ in the aerosol backscatter coefficient is observed. However, this period together with the peak of 20 April, 22:00 UTC correspond to the highest volcanic aerosol optical depth observed at CIAO with a value of 0.12 at 355 nm.

In terms of intensive properties, there is a significant difference respect to the other cases. Lidar ratio values are between those observed for the first arrival on 20 April and the conditions after 21 April, while Ångström exponents are smaller and a mean particle linear depolarization ratio of 16%, similar to 20 April case, is observed.

4.1.5 18–19 May 2010

The last observation of volcanic particles over Potenza was recorded on 18–19 May between 2 and 5 km a.s.l., when there was no block of the air traffic over Italy or alert for volcanic particle arrival. During the same days, the reported mask identifies layers above 5 km a.s.l. whose origin cannot be clearly identified at this stage. For these days, backtrajectories do not clearly indicate the volcanic origin of the observed particles, but pass over continental Europe and the Atlantic Ocean. We could assume that these are volcanic particles because starting from the first explosive eruption on 15 April we have observed volcanic aerosol traces at these altitudes. However, as far as this case is concerned, the lack of multi-wavelength analyses due both to the sparse low clouds (about 60% of the time) and diurnal conditions does not permit a reliable typing of these layers.

ACPD
11, 12763–12803, 2011

4.2 Overview of volcanic aerosol optical properties

The dependence of intensive properties retrieved by lidar on relative humidity measured (*RH*) by the co-located microwave radiometer is reported in Fig. 8. In particular, backscatter-related Ångström exponent at 532/1064 nm (Fig. 8a) and lidar ratio at 355 nm (Fig. 8c) are reported since more data are available respect to Ångström exponent at 532/355 nm and lidar ratio at 532 nm, respectively. The particle linear depolarization ratio is reported as a function of *RH* in Fig. 8b. In addition, the ratio of the lidar ratio at the 2 wavelengths is reported (Fig. 8d), since this parameter has been found to be important for the microphysical properties investigations (Müller et al., 2007).

The dependence on relative humidity of the backscatter-related Ångström exponent is the clear signature of the hygroscopic growth with the *RH* increase. A similar dependence on *RH* is found for the ratio of lidar ratios. The particle linear depolarization ratio shows on average a trend increasing with *RH*, that could indicate the presence of sulfate aerosols for the whole period (Sakai et al., 2000).

No clear *RH* dependence is found for S_{uv}: for the same *RH* value, low (around 40 sr) and high (around 85 sr) values are observed. In particular, low lidar ratio values are measured on 20 April. The S_{uv} value of 54 sr recorded for the same event on 19 April indicates an increase with *RH* for this specific event. The observations collected at CIAO from 19 to 20 April correspond both to the largest amount of transportable ash emitted by the volcano and the highest maximum emission height ranges (Matthias et al., 2011). On 13 May a similar situation is found in terms of transportable emitted aerosol and emission altitude. Indeed, these days are related to the strongest peaks, decreasing with the altitude, revealed in the temporal evolution of backscatter profiles. In addition, S_{uv} mean value measured in the volcanic layer on 13 May fits well with the S_{uv} dependence on *RH* observed for the 19–20 April data. This suggests differences in terms of the microphysical properties of volcanic particles reaching CIAO on 19–20 April and 13 May respect to the other days.

On 19–20 April and 13 May 2010, it can be observed a larger amount of aerosol emitted by the Icelandic volcano characterized by a lidar ratio of about 40 sr at 355 nm increasing with the relative humidity up to 60–70 sr, and a ratio of lidar ratios of about 0.8. Lidar ratio values around 55 sr are reported in literature for fresh ash cases (Pappalardo et al., 2004; Ansmann et al., 2010). This suggests the presence of some ash, besides sulfates, also in agreement with higher backscatter-related Ångström exponents for the same *RH* on these days respect to all the other cases (see Fig. 8a). Moreover, there are some indications that the aging of aerosol through the European continent could affect the ratio of lidar ratios so as to lead this to values below 1 (Müller at al., 2007). In addition, the 19–20 April and 13 May cases correspond to the observation of ultra-giant particles signature in the cloud radar signals (Madonna et al., 2010b), furthermore confirming the different microphysical properties of the volcanic particles observed on these days.

For all the other cases, 80 sr is obtained as lidar ratio in UV and the ratio of lidar ratios is greater than 1. This could be related to more mixing with continental and sulfates aerosol, in agreement with high S_{uv}, enlarged particles and the values of the ratio of lidar ratios (Ansmann et al., 2011; Müller et al., 2007).

At this stage the aerosol size distribution for the cases reported in Table 2 and Fig. 8 cannot be appropriately investigated on the basis of co-located AERONET measurements because of the high variability observed in the aerosol content and typing (Fig. 1 and 7), the no simultaneous Raman lidar (night-time) and co-located AERONET sunphotometer (diurnal) measurements and the few AERONET data available due to the presence of clouds. A devoted study based both on the integration of lidar-radar measurements, with the support of all ancillary instrumentations available at CIAO, and a numerical simulation will be carried out in order to investigate the aerosol size and microphysical properties of these volcanic observations in depth.

ACPD
11, 12763–12803, 2011

5 Summary

The observations of Eyjafjallajökull volcanic cloud by multi-wavelength Raman lidar performed at CIAO observatory, in Southern Italy, are presented and discussed. These measurements can be a reference point for the investigation of the sensitivity of transport model due both to the long source-observational point distance and the low amount of volcanic aerosol reaching this area.

A methodology for the identification of the volcanic layer starting from temporal series of quality assured particle backscatter profiles is described into details. With the support of model outputs, this methodology relies both on the multi-wavelength Raman lidar measurements and the long-term measurements performed at CIAO within EARLINET. The described methodology will be applied to all the EARLINET measurements performed during the Eyjafjallajökull eruption in 2010 (Pappalardo et al., 2011).

The aerosol masking for the 19 April–20 May period shows that volcanic aerosol are observed at CIAO in 4 periods: 19–22 April, 27–29 April, 8–9 May, 13–14 May and 18–19 May. Volcanic layers are observed in the whole troposphere, with intrusions in the PBL on 21–22 April and 13 May. The co-presence of dust and volcanic aerosol is observed both at different levels and mixed with the same layer.

Two maxima of about 0.12–0.13 are found for volcanic layer aerosol optical depth at 355 nm on 20 April, 22:00 UTC and 13 May, 20:30 UTC. These values are significantly lower than the peak values up to 0.7 observed during Saharan dust events at the same location (Mona et al., 2006b) and, in spite of the larger distance from the Eyjafjallajökull volcano, they are comparable to what was observed at CIAO during the Etna eruption in 2002.

A complete multi-wavelength analysis of the long-range transported volcanic aerosol is presented for the most significant time-windows. The dependence of lidar retrieved intensive properties on relative humidity is studied. High S_{uv}, particle linear depolarization ratio increasing with *RH* and values of the ratio of lidar ratios greater than 1 suggest the presence of volcanic sulfates/continental mixed aerosol. In correspondence of the

ACPD
11, 12763–12803, 2011

peaks in the observed volcanic aerosol AOD, the lidar ratio increasing with *RH* from about 40 sr at 20% as *RH* up to about 70 sr at *RH* of about 70% and the ratio of lidar ratio values below 1 suggest the presence, besides sulfates aerosols, of some ash affected by the aging through the European continent. A devoted study based on the synergic use of all CIAO observatory instrumentations and in particular on lidar-radar integration will be carried out in order to investigate the aerosol size and microphysical properties for these volcanic observations in depth.

Acknowledgements. The financial support for EARLINET by the European Commission under grant RICA-025991 is gratefully acknowledged. We acknowledge the support of the European Commission through GEOmon Integrated Project under the 6th Framework Programme (contract number FP6-2005-Global-4-036677). The CIAO observatory is partially supported by the Italian Civil Protection Department of the Ministry Council.

Authors would like to thank the NOAA Air Resources Laboratory (ARL) for the provision of the HYSPLIT backtrajectory analysis; the German Weather Service for the air mass back-trajectory analysis, NILU for providing FLEXTRA back-trajectories based on meteorological data provided from ECMWF (European Centre for Medium Range Weather Forecast)and available at http://www.nilu.no/trajectories; and Tom L. Kucsera (GEST) at NASA/Goddard for back-trajectories available at the aeronet.gsfc.nasa.gov website. We also thank the Barcelona Supercomputing Center for forecasts with the Dust Regional Atmospheric Model (DREAM) and the Data User Element of the European Space Agency Data for data available from “ATSR World Fire Atlas”. The Eyjafjallajökull volcanic activity was monitored through updated reports provided by the Iceland Meteorological Office and available at http://en.vedur.is/earthquakes-and-volcanism/articles/nr/2072.

References

Ansmann, A., Riebesell, M., Wandinger, U., Weitkamp, C., Voss, E., Lahmann, W., and Michaelis, W.: Combined Raman elastic-backscatter lidar for vertical profiling of moisture, aerosol extinction, backscatter and lidar ratio, Appl. Phys. B., 55, 18–28, 1992.

Ansmann, A., Tesche, M., Groß, S., Freudenthaler, V., Seifert, P., Hiebsch, A., Schmidt, J., Wandinger, U., Mattis, I., Müller, D., and Wiegner M.: The 16 April 2010 ma-

ACPD
11, 12763–12803, 2011

jor volcanic ash plume over central Europe: EARLINET lidar and AERONET photometer observations at Leipzig and Munich, Germany, Geophys. Res. Lett., 37, L13810, doi:10.1029/2010GL043809, 2010.

Ansmann, A., Tesche M., Seifert P., Groß, S., Freudenthaler, V., Apituley, A., Wilson, K. M., Serikov, I., Linné, H., Heinold, B., Hiebsch, A., Schnell, F., Schmidt, J., Mattis, I., Wandinger, U., and Wiegner, M.: Ash and finemode particle mass profiles from EARLINETAERONET observations over central Europe after the eruptions of the Eyjafjallajökull volcano in 2010, J. Geophys. Res., doi:10.1029/2010JD015567, in press, 2010.

Böckmann, C., Wandinger, U., Ansmann, A., Bösenberg, J., Amiridis, V., Boselli, A., Delaval, A., De Tomasi, F., Frioud, M., Grigorov, I., Hågård, A., Horvat, M., Iarlori, M., Komguem, L., Kreipl, S., Larchevêque, G., Matthias, V., Papayannis, A., Pappalardo, G., Rocadenbosch, F., Rodrigues, J. A., Schneider, J., Shcherbakov, V., and Wiegner M.: Aerosol lidar intercomparison in the framework of the EARLINET project, 2. Aerosol backscatter algorithms, Appl. Opt., 43, 977–989, 2004.

Di Girolamo, P., Ambrico, P. F., Amodeo, A., Boselli, A., Pappalardo, G., and Spinelli, N.: Aerosol observations by lidar in the nocturnal boundary layer, Appl. Opt., 38(21), 4585–4595, 1999.

Draxler, R. R. and Rolph, G. D.: HYSPLIT (HYbrid Single-Particle Lagrangian Integrated Trajectory) Model access via NOAA ARL READY Website (http://ready.arl.noaa.gov/HYSPLIT.php). NOAA Air Resources Laboratory, Silver Spring, MD, 2011.

Emeis, S., Forkel, R., Junkermann, W., Schäfer, K., Flentje, H., Gilge, S., Fricke, W., Wiegner, M., Freudenthaler, V., Groß, S., Ries, L., Meinhardt, F., Birmili, W., Münkel, C., Obleitner, F., and Suppan, P.: Measurement and simulation of the 16/17 April 2010 Eyjafjallajökull volcanic ash layer dispersion in the northern Alpine region, Atmos. Chem. Phys., 11, 2689–2701, doi:10.5194/acp-11-2689-2011, 2011.

Flentje, H., Claude, H., Elste, T., Gilge, S., Köhler, U., Plass-Dülmer, C., Steinbrecht, W., Thomas, W., Werner, A., and Fricke, W.: The Eyjafjallajökull eruption in April 2010 – detection of volcanic plume using in-situ measurements, ozone sondes and lidar-ceilometer profiles, Atmos. Chem. Phys., 10, 10085–10092, doi:10.5194/acp-10-10085-2010, 2010.

Freudenthaler, V., Esselborn, M., Wiegner, M., Heese, B., Tesxhe, M., Ansmann, A., Müller, D., Althausen, D., Wirth, M., Fix, A., Ehret, G., Knippertz, P., Toledano, C., Gasteiger, J., Garhammer, M., and Seefeldner, M.: Depolarization ratio profiling at several wavelengths in pure Saharan dust during SAMUM 2006, Tellus B, 61, 165–179, doi:10.1111/j.1600-0889.2008.00396.x, 2009.

ACPD
11, 12763–12803, 2011

Lidar observations of the Eyjafjallajkull volcanic cloud over Southern Italy

L. Mona et al.

Gasteiger, J., Groß, S., Freudenthaler, V., and Wiegner, M.: Volcanic ash from Iceland over Munich: mass concentration retrieved from ground-based remote sensing measurements, Atmos. Chem. Phys., 11, 2209–2223, doi:10.5194/acp-11-2209-2011, 2011.

Langmann, B., Folch, A., Hensch, M., and Matthias, V.: Volcanic ash over Europe during the eruption of Eyjafjallajökull on Iceland, April–May 2010, Atmos. Environ., accepted, 2011.

Lettino, A., Caggiano R., Fiore S., Macchiato M., Sabia S., and Trippetta S.: Eyjafjallajökull volcanic ash in Southern Italy, Eyjafjallajökull special issue, Atmos. Environ., submitted, 2011.

Madonna, F., Amodeo, A., Boselli, A., Cornacchia, C., D'Amico, G., Giunta, A., Mona, L., Pappalardo, G., and Cuomo, V.: CIAO: the CNR-IMAA advanced observatory for atmospheric research, Atmos. Meas. Tech. Discuss., 3, 5253–5293, doi:10.5194/amtd-3-5253-2010, 2010a.

Madonna, F., Amodeo, A., D'Amico, G., Mona, L., and Pappalardo, G.: Observation of non-spherical ultragiant aerosol using a microwave radar, Geophys. Res. Lett., 37, L21814, doi:10.1029/2010GL044999, 2010b.

Matthias, V., Balis, D., Bösenberg, J., Eixmann, R., Iarlori, M., Komguem, L., Mattis, I., Papayannis, A., Pappalardo, G., Perrone, M. R., and Wang, X.: The vertical aerosol distribution over Europe: statistical analysis of Raman lidar data from 10 EARLINET stations, J. Geophys. Res., 109, D18201, doi:10.1029/2004JD004638, 2004.

Matthias, V., Aulingera, A., Biesera, J., Cuesta, J., Geyera, B., Langmanne, B., Serikov, I., Mattis, I., Minikin, A., Mona, L., Quante, M., Schumann, U., and Weinzierl, B.: The ash dispersion over Europe during the Eyjafjallajökull eruption – comparison of CMAQ simulations to remote sensing and in-situ observations, Atmos. Environ., submitted, 2011.

Mona, L., Amodeo, A., D'Amico, G., Pandolfi, M., and Pappalardo, G.: Lidar ratio climatology: 5 years of systematic Raman lidar measurements over Potenza, Italy – 23rd International Laser Radar Conference, Nara Japan, 24–28 July 2006, 1, 321–324, 2006a.

Mona, L., Amodeo, A., Pandolfi, M., and Pappalardo, G.: Saharan dust intrusions in the Mediterranean area: Three years of Raman lidar measurements, J. Geophys. Res., 111, D16203, doi:10.1029/2005JD006569, 2006b.

Mona, L., Cornacchia C., D'Amico G., Di Girolamo, P., Pappalardo, G., Pisani, G., Summa, D., Wang, X., and Cuomo, V.: Characterization of the variability of the humidity and cloud fields as observed from a cluster of ground-based lidar systems, Q. J. R. Meteorol. Soc., 133, (S3) 257–271, 2007.

ACPD

11, 12763–12803, 2011

Lidar observations of the Eyjafjallajkull volcanic cloud over Southern Italy

L. Mona et al.

Mona, L., Pappalardo, G., Amodeo, A., D'Amico, G., Madonna, F., Boselli, A., Giunta, A., Russo, F., and Cuomo, V.: One year of CNR-IMAA multi-wavelength Raman lidar measurements in coincidence with CALIPSO overpasses: Level 1 products comparison, Atmos. Chem. Phys., 9, 7213–7228, doi:10.5194/acp-9-7213-2009, 2009.
Morille, Y., Haeffelin, M., Drobinski, P., and Pelon, J.: STRAT: An Automated Algorithm to Retrieve the Vertical Structure of the Atmosphere from Single-Channel Lidar Data, Jour. Atm. Ocean. Tech, 24, 761–775, 2007.
Müller, D., Ansmann A., Mattis I., Tesche M., Wandinger U., Althausen, D., and Pisani, G.: Aerosol-type-dependent lidar ratio observed with Raman lidar. J. Geophys. Res., 112, D16202, doi:10.1029/2006JD008292, 2007.
Müller, D., Heinold, B., Tesche, M., Tegen, I., Althausen, D., Alados Arboledas, L., Amiridis, V., Amodeo, A., Ansmann, A., Balis, D., Comeron, A., D'Amico, G., Gerasopoulos, E., Guerrero-Rascado, J. L., Freudenthaler, V., Giannakaki, E., Heese, B., Iarlori, M., Knippertz, P., Mamouri, R. E., Mona, L., Papayannis, A., Pappalardo, G., Perrone, R.-M., Pisani, G., Rizi, V., Sicard, M., Spinelli, N., Tafuro, A., and Wiegner, M.: EARLINET observations of the 14–22-May long-range dust transport event during SAMUM 2006: validation of results from dust transport modelling, Tellus, 61B, 325–339, 2009.
Papayannis, A., Amiridis, V., Mona, L., Tsaknakis, G., Balis Bösenberg J., Chaikovski, A., De Tomasi, F., Grigorov, I., Mattis, I., Mitev, V., Müller, D., Nickovic, S., Pérez, C., Pietruczuk, A., Pisani, G., Ravetta, F., Rizi, V., Sicard, M., Trickl, T., Wiegner, M., Gerding, M., D'Amico, G., and Pappalardo, G.: Systematic lidar observations of aerosol optical properties during Saharan dust intrusions over Europe, in the frame of EARLINET (2000–2002): Statistical analysis and results, J. Geophys. Res., 113, D10204, doi:10.1029/2007JD009028, 2008.
Pappalardo, G., Amodeo, A., Pandolfi, M., Wandinger, U., Ansmann, A., Bosenberg, J., Matthias, V., Amiridis, V., De Tomasi, F., Frioud, M., Iarlori, M., Komguem, L., Papayannis, A., Rocadenbosch, F., and Wang, X.: Aerosol lidar intercomparison in the framework of the EARLINET project. 3. Raman lidar algorithm for aerosol extinction, backscatter and lidar ratio, Appl. Opt., 43, 5370–5385, 2004.
Pappalardo, G., Amodeo, A., Ansmann, A., Apituley, A., Alados Arboledas, L., Balis, D., Böckmann, C., Chaikovsky, A., Comeron, A., D'Amico, G., De Tomasi, F., Freudenthaler, V., Giannakaki, E., Giunta, A., Grigorov, I., Gustafsson, O., Gross, S., Haeffelin, M., Iarlori, M., Kinne, S., Linné, H., Madonna, F., Mamouri, R., Mattis, I., McAuliffe, M., Molero, F., Mona, L., Müller, D., Mitev, V., Nicolae, D., Papayannis, A., Perrone, M. R., Pietruczuk, A., Pujadas,

ACPD
11, 12763–12803, 2011

Lidar observations of the Eyjafjallajkull volcanic cloud over Southern Italy

L. Mona et al.

M., Putaud, J.-P., Ravetta,F., Rizi, V., Serikov, I., Sicard, M., Simeonov, V., Spinelli, N., Stebel, K., Trickl, T., Wandinger, U., Wang, X., Wagner, F., and Wiegner, M.: EARLINET observations of the Eyjafjallajökull ash plume over Europe, in "Lidar Technologies, Techniques, and Measurements for Atmospheric Remote Sensing VI", Proceedings of SPIE, SPIE Remote Sensing 2010, Toulouse, 20–23 September 2010, 7832, 78320 pp., 2010a.

Pappalardo, G., Amodeo, A., Ansmann, A., Apituley, A., Alados Arboledas, L., Balis, D., Böckmann, C., Chaikovsky, A., Comeron, A., D'Amico, G., De Tomasi, F., Freudenthaler, V., Giannakaki, E., Giunta, A., Grigorov, I., Gustafsson, O., Gross, S., Haeffelin, M., Iarlori, M., Kinne, S., Linné, H., Madonna, F., Mamouri, R., Mattis, I., McAuliffe, M., Molero, F., Mona, L., Müller, D., Mitev, V., Nicolae, D., Papayannis, A., Perrone, M. R., Pietruczuk, A., Pujadas, M., Putaud, J.-P., Ravetta, F., Rizi, V., Serikov, I., Sicard, M., Simeonov, V., Spinelli, N., Stebel, K., Trickl, T., Wandinger, U., Wang, X., Wagner, F., and Wiegner, M.: Dispersion and evolution of the Eyjafjallajökull ash plume over Europe: vertically resolved measurements with the European LIDAR network EARLINET, 7th European Geosciences Union (EGU) General Assembly 2010, Vienna, Austria, 02–07 May 2010, EGU2010-15731, 2010b.

Pappalardo, G., Wandinger, U., Mona, L., Hiebsch, A., Mattis, I., Amodeo, A., Ansmann, A., Seifert, P., Linné, H., Apituley, A., Alados Arboledas, L., Balis, D., Chaikovsky, A., D'Amico, G., De Tomasi, F., Freudenthaler, V., Giannakaki, E., Giunta, A., Grigorov, I., Iarlori, M., Madonna, F., Mamouri, R.-E., Nasti, L., Papayannis, A., Pietruczuk, A., Pujadas, M., Rizi, V., Rocadenbosch, F., Russo, F., Schnell, F., Spinelli, N., Wang, X., and Wiegner, M.: EARLINET correlative measurements for CALIPSO: First intercomparison results, J. Geophys. Res., 115, D00H19, doi:10.1029/2009JD012147, 2010c.

Pappalardo, G., Mona, L., Adam, M., Apituley, A., Arboledas, L. A., Chaikovsky, A., Cuesta, J., de Tomasi, F., D'Amico, G., Giannakaki, E., Grigorov, I., Gross, S., Iarlori, M., Mamouri, R. E., Mattis, I., Mitev, V., Nicolae, D., Pietruczuk, A., Serikov, I., Sicard, M., Simenov, V., Spinelli, N., Trickl, T., and Wagner, F.: 4D distribution of the 2010 Eyjafjallajökull volcanic cloud over Europe observed by EARLINET, Atmos. Chem. Phys., in preparation, 2011.

Petersen, G. N.: A short meteorological overview of the Eyjafjallajökull eruption 14 April–23 May 2010, Weather, 65, 203–207, doi:10.1002/wea.634, 2010.

Sakai, T., Shibata, T., Kwon, S., Kim, Y., Tamura, K., and Iwasaka, Y.: Free tropospheric aerosol backscatter, depolarization ratio, and relative humidity measured with the Raman lidar at Nagoya in 1994–1997: contributions of aerosols from the Asian Continent and the Pacific Ocean, Atmos. Environ., 34, 431–442, 2000.

ACPD
11, 12763–12803, 2011

Schoeberl, M. R. and Newman, P. A.: A multiple-level trajectory analysis of vortex filaments, J. Geophys. Res., 100, 25801–25816, 1995.
Schumann, U., Weinzierl, B., Reitebuch, O., Schlager, H., Minikin, A., Forster, C., Baumann, R., Sailer, T., Graf, K., Mannstein, H., Voigt, C., Rahm, S., Simmet, R., Scheibe, M., Lichtenstern, M., Stock, P., Rüba, H., Schäuble, D., Tafferner, A., Rautenhaus, M., Gerz, T., Ziereis, H., Krautstrunk, M., Mallaun, C., Gayet, J.-F., Lieke, K., Kandler, K., Ebert, M., Weinbruch, S., Stohl, A., Gasteiger, J., Groß, S., Freudenthaler, V., Wiegner, M., Ansmann, A., Tesche, M., Olafsson, H., and Sturm, K.: Airborne observations of the Eyjafjalla volcano ash cloud over Europe during air space closure in April and May 2010, Atmos. Chem. Phys., 11, 2245–2279, doi:10.5194/acp-11-2245-2011, 2011.
Steyn, D., Baldi G. M., and Hoff R. M.: The Detection of Mixed Layer Depth and Entrainment Zone Thickness from Lidar Backscatter Profiles, J. Atmos. Ocean. Tech., 16(7), 953–959, 1999.
Stohl, A.: Computation, accuracy and applications of trajectories – a review and bibliography, Atmos. Environ., 32, 947–966, 1998.
Stohl, A. and Seibert, P.: Accuracy of trajectories as determined from the conservation of meteorological tracers, Q. J. Roy. Met. Soc., 124, 1465–1484, 1998.
Stohl, A., Wotawa, G., Seibert, P., and Kromp-Kolb, H.: Interpolation errors in wind fields as a function of spatial and temporal resolution and their impact on different types of kinematic trajectories, J. Appl. Meteor., 34, 2149–2165, 1995.
Stohl, A., Prata, A. J., Eckhardt, S., Clarisse, L., Durant, A., Henne, S., Kristiansen, N. I., Minikin, A., Schumann, U., Seibert, P., Stebel, K., Thomas, H. E., Thorsteinsson, T., Tørseth, K., and Weinzierl, B.: Determination of time- and height-resolved volcanic ash emissions for quantitative ash dispersion modeling: the 2010 Eyjafjallajökull eruption, Atmos. Chem. Phys. Discuss., 11, 5541–5588, doi:10.5194/acpd-11-5541-2011, 2011.
Vaughan, M., Young, S., Winker, D., Powell, K., Omar, A., Liu, Z., Hu, Y., and Hostetler, C.: Fully automated analysis of space-based lidar data: an overview of the CALIPSO retrieval algorithms and data products, in “Laser Radar Techniques for Atmospheric Sensing”, Proceedings of SPIE, SPIE 2004, Bellingham, WA, USA, 5575, doi:10.1117/12.572024, 2004.
Villani, M. G., Mona, L., Maurizi, A., Pappalardo, G., Tiesi, A., Pandolfi, M., D’Isidoro, M., Cuomo, V., and Tampieri, F.: Transport of volcanic aerosol in the troposphere: the case study of the 2002 Etna plume, J. Geophys. Res., 111, D21102, doi:10.1029/2006JD007126, 2006.

ACPD
11, 12763–12803, 2011

Wang, L. and Sassen, K.: Wavelet Analysis of Cirrus Multiscale Structures from Lidar Backscattering: A Cirrus Uncinus Complex Case Study, J. Appl. Meteorol. Clima., 47(10), 2645–2658, doi:10.1175/2008JAMC1788.1, 2008.

ACPD

11, 12763–12803, 2011

Table 1. Intensive properties calculated within identified volcanic layers. Mean values and standard deviations of the lidar ratio at 355 nm (S_{uv}) and 532 nm (S_{vis}); Ångström exponent at 355/532 nm (å(α)); backscatter related Ångström exponent at 532/1064 nm (å(β)) and particle linear depolarization ratio at 532 nm (δ) are reported.

Hour (UTC)	Altitude [km a.s.l.]	S_{uv} [sr]	S_{vis} [sr]	å(α)	å(β)	δ
19:53–20:24 19 April	2.1–4.2	54 ± 14	n.a.	n.a.	n.a.	n.a.
21:00–23:05 20 April	2–3 3.1–4	42 ± 2 38 ± 6	50 ± 3 n.a.	1.4 ± 0.2 n.a.	1.8 ± 0.1 1.7 ± 0.1	0.15 ± 0.03 0.22 ± 0.03
11:30–12:30 21 April	1.6–3.6	n.a.	n.a.	n.a.	1.3 ± 0.7	n.a.
19:07–03:09 21–22 April	1.6–3.4	80 ± 12	78 ± 13	1.1 ± 0.3	1.21 ± 0.07	0.25 ± 0.05
22:17–23:24 29 April	2.7–3.4	80 ± 17	92 ± 16	1.4 ± 0.3	1.39 ± 0.04	n.a.
19:03–21:58 09 May	1.6–2.5 2.5–5	89 ± 11 n.a.	78 ± 15 n.a.	1.03 ± 0.07 n.a.	1.5 ± 0.6 2.1 ± 0.5	0.14 ± 0.04 0.10 ± 0.09
20:16–21:01 13 May	1.5–2.3 2.3–2.6	60 ± 11 60 ± 7	78 ± 12 n.a.	1.1 ± 0.4 n.a.	0.82 ± 0.03 1.04 ± 0.07	0.16 ± 0.07 n.a.

ACPD
11, 12763–12803, 2011

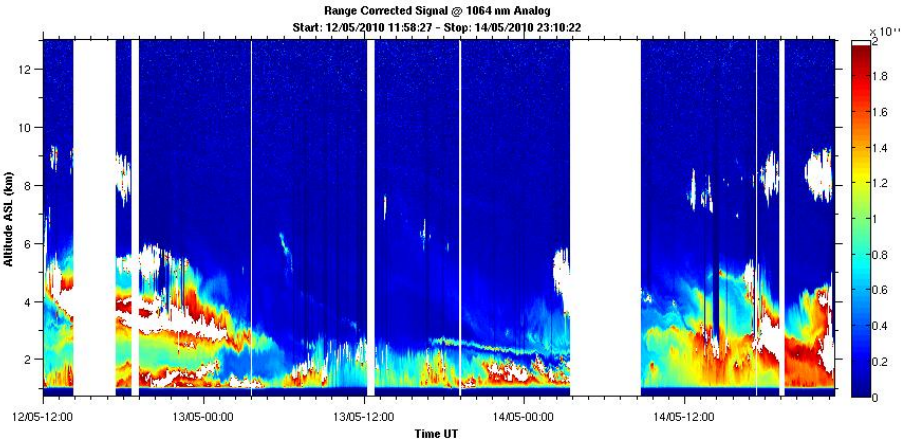

Fig. 1. Temporal evolution of range corrected lidar signal measured at 1064 nm in the 12–14 May period by PEARL at CIAO. The vertical and temporal resolutions are respectively 7.5 m and 30 s.

ACPD
11, 12763–12803, 2011

Lidar observations of the Eyjafjallajkull volcanic cloud over Southern Italy

L. Mona et al.

Title Page
Abstract | Introduction
Conclusions | References
Tables | Figures
◄ | ►
Back | Close
Full Screen / Esc
Printer-friendly Version
Interactive Discussion

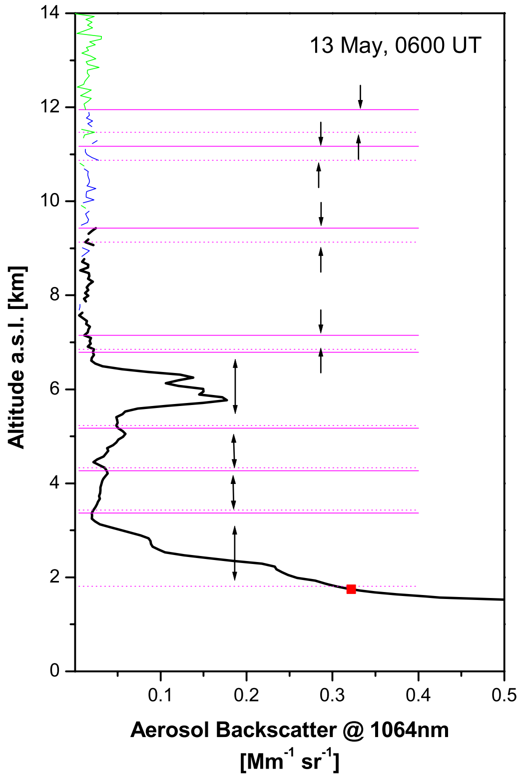

Fig. 2. Example of single profile particle layer identification as performed on the aerosol backscatter profile at 1064 nm measured on 13 May, at 05:30–06:30 UTC. Horizontal dotted and solid lines indicate the base and top of the identified layers, respectively. Red square indicates the PBL top height. Region with relative errors between 30–50% are reported in blue and those with relative error exceeding 50% in green.

ACPD
11, 12763–12803, 2011

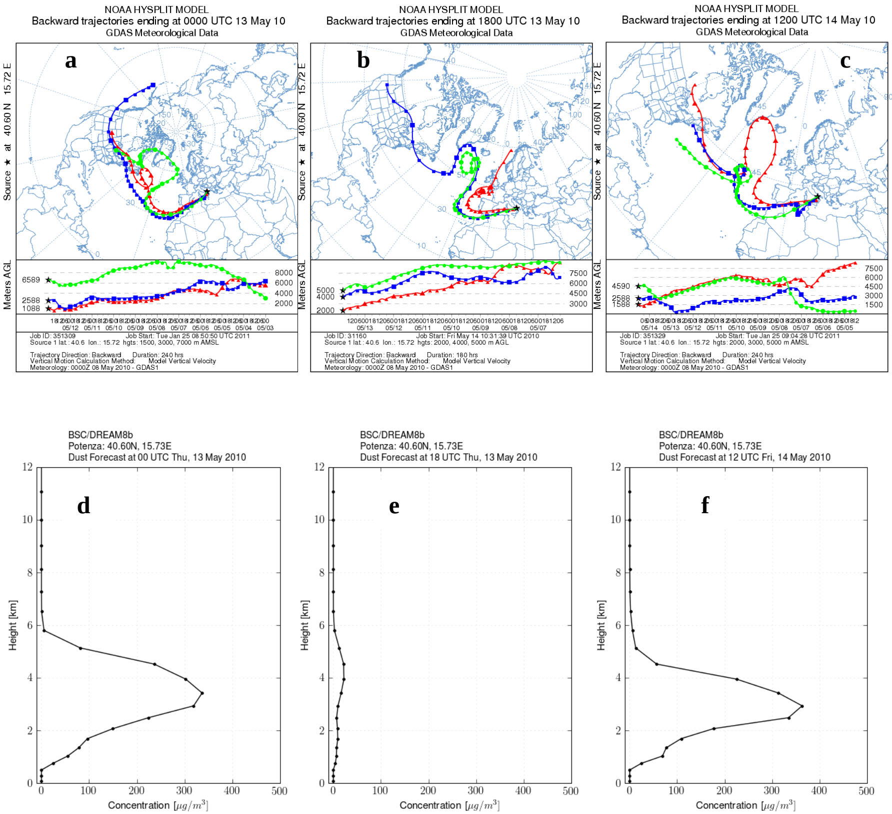

Fig. 3. HYSPLIT backtrajectory analysis (upper panel) and DREAM forecast vertical profiles of dust concentration (lower panel) for 13 May, 00:00 UTC **(a, d)**, 13 May, 18:00 UTC **(b, e)** and 14 May, 12:00 UTC **(c, f)**. Altitude layers at arrival point in the backtrajectory analysis are chosen accordingly to the layers identified through the method reported in Sect. 3.1.

ACPD
11, 12763–12803, 2011

Lidar observations of the Eyjafjallajkull volcanic cloud over Southern Italy

L. Mona et al.

Title Page
Abstract Introduction
Conclusions References
Tables Figures
◀◀ ▶▶
◀ ▶
Back Close
Full Screen / Esc
Printer-friendly Version
Interactive Discussion

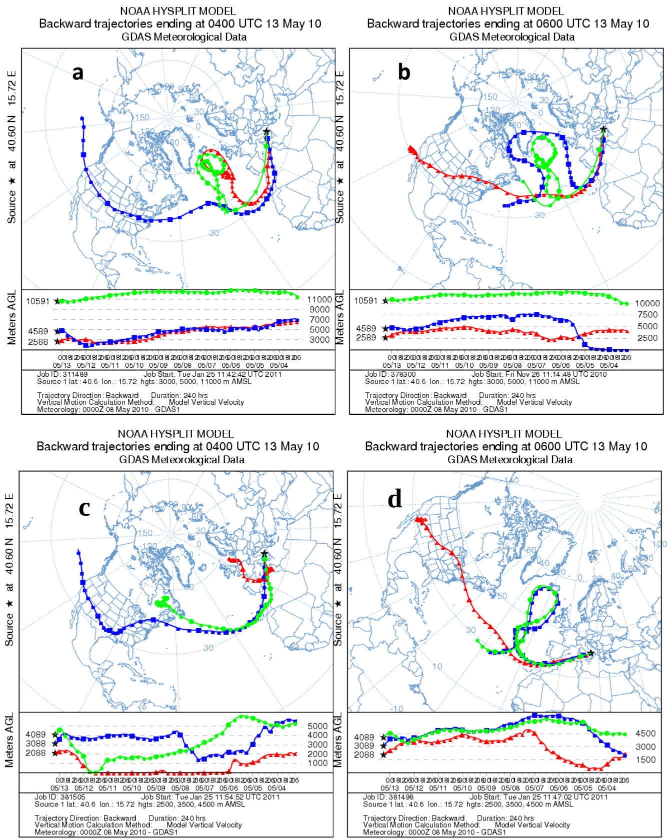

Fig. 4. Examples of HYSPLIT backtrajectory analysis in correspondence of transition regime between Saharan dust observation and the volcanic aerosol arrival on 13 May 2010, around 05:00 UTC. Altitudes at arrival point in the backtrajectory analysis are chosen accordingly to the layers identified through Sect. 3.1 reported method.

ACPD
11, 12763–12803, 2011

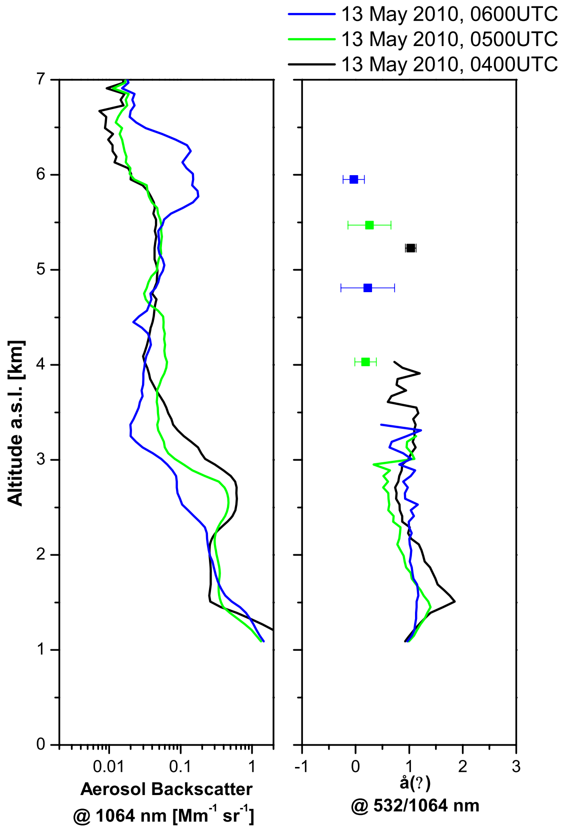

Fig. 5. Profiles of the aerosol backscatter at 1064 nm and of the backscatter related Ångström exponent at 532/1064 nm measured on 13 May, at 04:00, 05:00 and 06:00 UTC. Mean values are reported as squares for backscatter related Ångström exponent at altitude levels where corresponding profile is highly noisy. Error bars report the standard errors for the mean values.

ACPD
11, 12763–12803, 2011

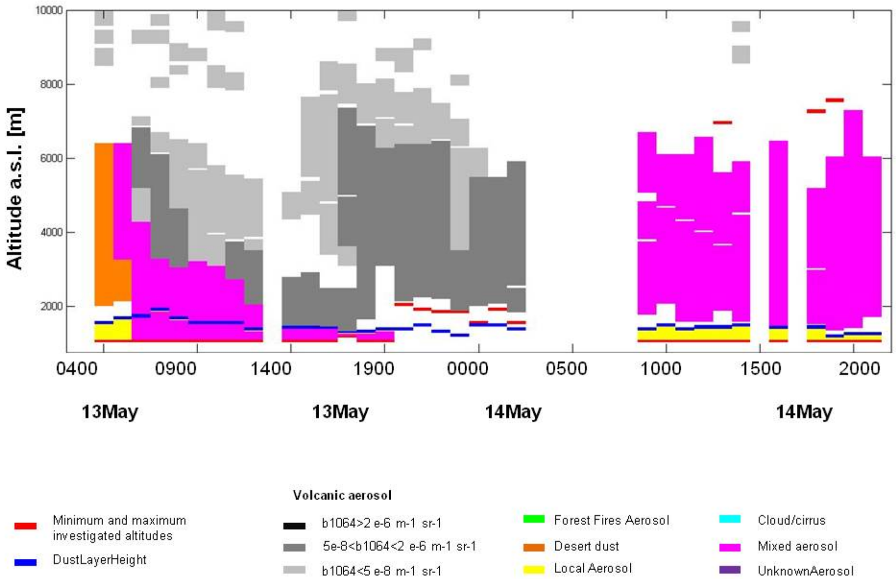

Fig. 6. Aerosol mask for the 13–14 May 2010 case as obtained by the methodology reported in this section. Only the time window affected by volcanic aerosol is included.

ACPD
11, 12763–12803, 2011

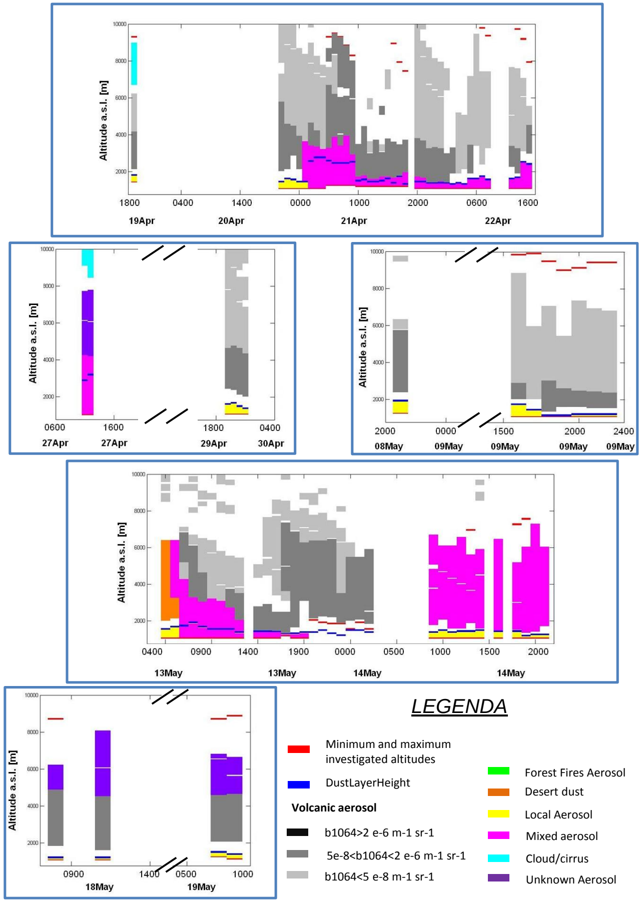

Fig. 7. Aerosol masks related to the whole volcanic period are reported in chronological order from the top to the bottom.

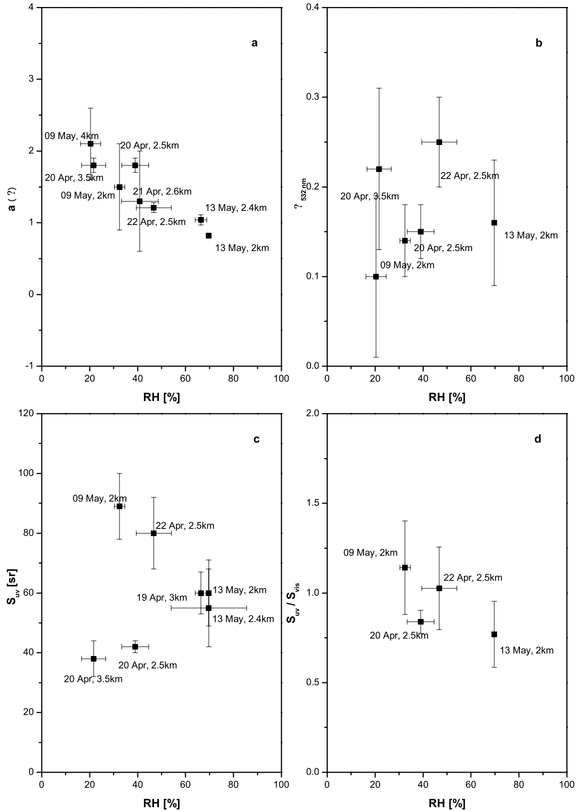

Fig. 8. Intensive properties calculated with identified volcanic layers are reported as a function of the relative humidity as measured by the co-located microwave profiler. The backscatter related Ångström exponent at 532/1064 nm (å(β)), the lidar ratio at 355 nm (S_{uv}), the ratio of lidar ratios (S_{uv}/S_{vis}), and the particle linear depolarization ratio at 532 nm (δ) are reported respectively in panel **a, b, c** and **d**. Standard deviations are reported as error bars.

ACPD
11, 12763–12803, 2011